

1 **Engineered bacteria detect tumor DNA**

2

3 Robert M. Cooper<sup>1\*</sup>, Josephine A. Wright<sup>2,\*</sup>, Jia Q. Ng<sup>3</sup>, Jarrad M. Goyne<sup>2</sup>, Nobumi  
4 Suzuki<sup>2,3</sup>, Young K. Lee<sup>3</sup>, Mari Ichinose<sup>2,3</sup>, Georgette Radford<sup>3</sup>, Elaine M. Thomas<sup>3</sup>, Laura  
5 Vrbanac<sup>3</sup>, Rob Knight<sup>6,7,8,9</sup>, Susan L. Woods<sup>2,3,\*\*</sup>, Daniel L. Worthley<sup>2,4,\*\*</sup> and Jeff  
6 Hasty<sup>1,5,6,9\*\*</sup>.

7

8 1. BioCircuits Institute, University of California, San Diego, La Jolla, CA, USA

9 2. Precision Medicine Theme, South Australia Health and Medical Research Institute,  
10 Adelaide, SA, Australia.

11 3. University of Adelaide, Adelaide, SA, Australia

12 4. Colonoscopy Clinic, Brisbane, Qld, Australia.

13 5. Department of Bioengineering, University of California, San Diego, La Jolla, CA.

14 6. Molecular Biology Section, Division of Biological Sciences, University of California,  
15 San Diego, La Jolla, CA, USA.

16 7. Department of Pediatrics, University of California, San Diego, La Jolla, CA.

17 8. Department of Computer Science & Engineering, University of California, San Diego,  
18 La Jolla, CA.

19 9. Center for Microbiome Innovation, University of California, San Diego, La Jolla, CA.

20 \* These authors contributed equally

21 \*\* Corresponding authors

22

23

24

25 **Word count:**

26 Summary paragraph = 228 words

27 The main text (summary paragraph plus body text) = 2076 words

28

## 29 Summary

30  
31 Advances in bacterial engineering have catalysed the development of living cell  
32 diagnostics and therapeutics<sup>1-3</sup>, including microbes that respond to diseases such as gut  
33 inflammation<sup>4</sup>, intestinal bleeding<sup>5</sup>, pathogens<sup>6</sup> and hypoxic tumors<sup>7</sup>. Bacteria can easily  
34 access the entire gastrointestinal tract via oral administration<sup>8</sup>, and they can produce  
35 outputs that can be noninvasively measured in stool<sup>4</sup> or urine<sup>7</sup>. Cellular memory, such as  
36 bistable switches<sup>4,9,10</sup> or genomic rearrangement<sup>11</sup>, has been used to allow bacteria to store  
37 information over time. However, living biosensors have not yet been engineered to detect  
38 specific DNA sequences or mutations from outside the cell. Here, we engineer naturally  
39 competent *Acinetobacter baylyi* to detect donor DNA from the genomes of colorectal  
40 cancer (CRC) cells and organoids. We characterize the functionality of the biosensors *in*  
41 *vitro* with co-culture assays and then validate *in vivo* with sensor bacteria delivered orally  
42 or rectally into mice injected with orthotopic donor CRC organoids. We observe  
43 horizontal gene transfer from the tumor to the sensor bacteria *in vivo*, allowing their  
44 detection in stool. The sensor bacteria achieved 100% discrimination between mice with  
45 and without CRC using both delivery methods. Our findings establish a framework for  
46 biosensing applications that require the detection of mutations or organisms within  
47 environments that are difficult to sample. In addition, the platform can be readily  
48 expanded to include *in situ* production and delivery of therapeutic payloads at the  
49 detection site.

## 51 Main text

52  
53 Some bacteria are naturally competent for transformation and can sample extracellular  
54 DNA directly from their environment<sup>12</sup>. Natural competence is one mechanism of  
55 horizontal gene transfer (HGT), the exchange of genetic material between organisms  
56 outside vertical, “parent to offspring” transmission<sup>13</sup>. HGT is common between microbes<sup>13</sup>  
57 and from microbes into animals and plants<sup>14</sup>. Genomic analyses have found signatures of  
58 HGT from eukaryotes to prokaryotes<sup>15</sup>, but the forward engineering of bacteria to detect  
59 or respond to human DNA via HGT has not been explored. *Acinetobacter baylyi* is a  
60 highly competent and well-studied bacterium<sup>16</sup> that is largely non-pathogenic in healthy  
61 humans<sup>17</sup> and can colonize the murine gastrointestinal tract<sup>18</sup>. This combination of traits  
62 renders *A. baylyi* an ideal candidate for engineered detection of target DNA *in situ* (Fig.  
63 1). Our strategy delivers bacterial biosensors non-invasively to the gastrointestinal tract,  
64 where they sample and genomically integrate target tumor DNA. To systematically  
65 demonstrate the concept, we use the sensor to detect engineered tumor cells. Since *A.*  
66 *baylyi* is easily transformable, our approach can be expanded to harness HGT to interact

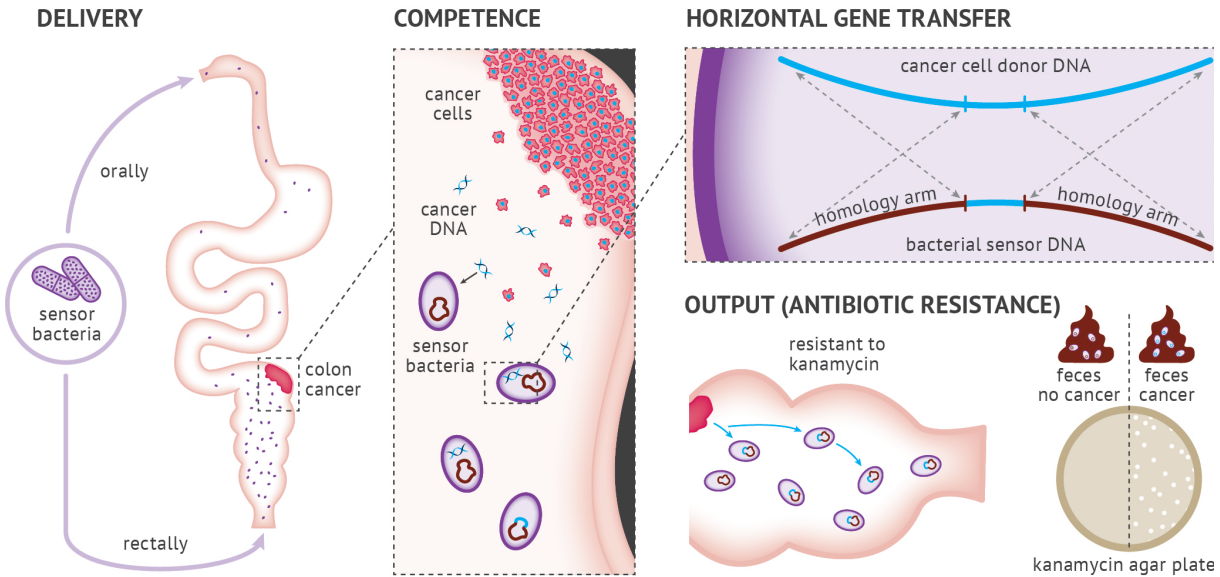


**Figure 1. Engineered bacteria to detect tumor DNA.** Engineered *A. baylyi* bacteria are delivered orally or rectally in an orthotopic mouse model of CRC. The naturally competent *A. baylyi* take up tumor DNA shed into the colonic lumen. The tumor donor DNA is engineered with a *kanR* cassette flanked by *KRAS* homology arms (HA). The sensor bacteria are engineered with matching *KRAS* homology arms that promote homologous recombination. Sensor bacteria that undergo HGT from tumor DNA, acquire kanamycin resistance and are quantified from stool by serial dilution on kanamycin selection plates.

67 with genetic elements within the sensor bacteria in a manner that activates downstream  
68 output.

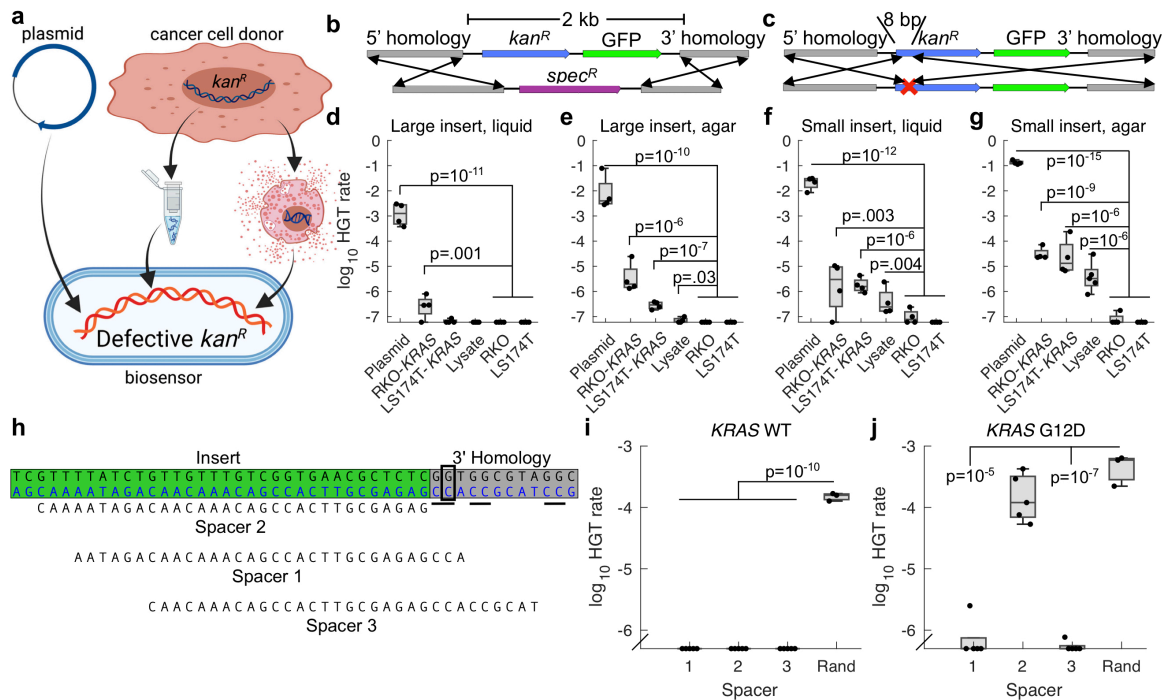
69

## 70 Sensor bacteria can detect human cancer DNA

71

72 To test the hypothesis that bacteria could detect human tumor DNA, we generated  
73 transgenic donor human cancer cells and sensor bacteria (Fig. 2a). The donor cassette  
74 comprised a kanamycin resistance gene and GFP (*kan<sup>R</sup>-GFP*) flanked by 1 kb homology  
75 arms from human *KRAS* (Fig. 2b-c and Extended Data Fig. 1). *KRAS* is an important  
76 oncogene in human cancer, and a driver mutation in *KRAS* often accompanies the  
77 progression of simple into advanced colorectal adenomas<sup>19</sup>. We stably transduced this  
78 donor cassette into both RKO and LS174T human CRC cell lines using a lentiviral vector.  
79 To construct the sensor bacteria, we inserted a complementary landing pad with *KRAS*  
80 homology arms into a neutral genomic site of *A. baylyi*. We tested both a “large insert”  
81 design (2 kb), with a different resistance marker between the *KRAS* arms to be replaced  
82 by the donor cassette (Fig. 2b, Extended Data Fig. 2a), and a “small insert” design (8  
83 bp), with the same *kan<sup>R</sup>-GFP* cassette as in the tumor donor DNA but interrupted by 2  
84 stop codons in *kan<sup>R</sup>* (Fig. 1 & 2c, Extended Data Fig. 2b & 3). The biosensor output was  
85 growth on kanamycin plates, measured as colony-forming units (CFUs).

86



87 We tested both designs using various donor DNA sources, both in liquid culture and on  
 88 solid agar (Fig. 2a). The “large insert” biosensors detected donor DNA from purified  
 89 plasmids and genomic DNA both in liquid (Fig. 2d) and on agar (Fig. 2e). On agar, they  
 90 also detected raw, unpurified lysate, albeit at just above the limit of detection (Fig. 2e).  
 91 As expected<sup>20</sup>, the “small insert” design improved detection efficiency roughly 10-fold,  
 92 reliably detecting donor plasmid, purified genomic DNA, and raw lysate both in liquid  
 93 and on agar (Fig. 2f-g, Extended Data Supplemental Movie). Across donor DNA and  
 94 biosensor design, detection on solid agar was approximately 10-fold more efficient than  
 95 in liquid culture. Importantly, detection of donor DNA from raw lysate demonstrated  
 96 that the biosensors do not require *in vitro* DNA purification<sup>21</sup>.

97  
 98 *A. baylyi* can take up DNA at approximately 60 bp/s<sup>22</sup>. Given a human genome of 3.2 x  
 99 10<sup>9</sup> bp, each *A. baylyi* cell, including its direct ancestors, can sample roughly 10<sup>-3</sup> of a  
 100 human genome in a 24-hour period. Combined with the data shown in Fig. 2g, with a  
 101 detection rate around 10<sup>-5</sup> per *A. baylyi* cell for RKO-*KRAS* and LS174T-*KRAS* donor

102 DNA, this suggests a detection efficiency of around 1% per processed donor sequence.  
103 While this calculation assumes a constant DNA processing rate, the result is quite similar  
104 to what we found for HGT from *E. coli* to *A. baylyi*<sup>21</sup>.

105

## 106 **Sensor bacteria can discriminate wild-type from mutant *KRAS* DNA**

107

108 Mutations in codon 12 of *KRAS* are present in 27% of CRC<sup>23</sup>, and are common in solid  
109 tumors generally<sup>24</sup>. To test whether sensor bacteria could discriminate between wild-type  
110 and mutant *KRAS* (*KRASG12D*), which differ by a single G>A transition, we utilized  
111 *A. baylyi*'s endogenous Type I-F CRISPR-Cas system<sup>25</sup>. We stably transduced an RKO  
112 cell line with the *kan<sup>R</sup>-GFP* donor cassette flanked by wild-type *KRAS* (RKO-*KRAS*),  
113 and a second line with *KRASG12D* flanking sequences (RKO-*KRASG12D*). Next, we  
114 designed 3 CRISPR spacers targeting the wild-type *KRAS* sequence at the location of  
115 the *KRASG12D* mutation, using the *A. baylyi* protospacer-adjacent motif (PAM) of 5'-  
116 CC-protospacer-3' (Fig. 2h). We inserted these as single-spacer arrays into a neutral locus  
117 in the "large insert" *A. baylyi* sensor genome.

118

119 The sensor bacteria, if effective, should reject wild-type *KRAS* through CRISPR-  
120 mediated DNA cleavage. Conversely, the *KRASG12D* sequence should alter the target  
121 sequence and evade DNA cleavage. Two of the three spacers blocked transformation by  
122 both wild-type and mutant DNA (Fig. 2i-j). However, spacer 2, for which the *KRASG12D*  
123 mutation eliminated the PAM site, selectively permitted HGT only with *KRASG12D*  
124 donor DNA (Fig. 2E-F). The other common mutations in codon 12 of *KRAS* all eliminate  
125 this PAM as well<sup>23</sup>. Thus, sensor *A. baylyi* can be engineered to detect a hotspot mutation  
126 in the *KRAS* gene with single-base specificity.

127

## 128 **Sensor bacteria can integrate cancer DNA in organoid culture**

129

130 *Ex vivo* organoid culture faithfully reflects endogenous tumor biology<sup>26</sup>. We therefore  
131 evaluated our sensor and donor constructs in organoid culture (Fig. 3a). We previously  
132 used CRISPR/Cas9 genome engineering to generate compound *Braf<sup>600E</sup>; Tgfbr2<sup>Δ/Δ</sup>*;  
133 *Rnf43<sup>Δ/Δ</sup>*; *Znrf3<sup>Δ/Δ</sup>*; *p16Ink4a<sup>Δ/Δ</sup>* (BTRZI) mouse organoids that recapitulate serrated  
134 CRC when injected into the mouse colon<sup>27</sup>.

135

136 We transduced BTRZI organoids with the human *KRAS*-flanked donor DNA construct  
137 (*KRAS-kan<sup>R</sup>*) to generate donor CRC organoids, and incubated their lysate with the more  
138 efficient "small insert" *A. baylyi* biosensors. As with the CRC cell lines, the sensor *A.*  
139 *baylyi* incorporated DNA from donor organoid lysate, but not from control lysates from



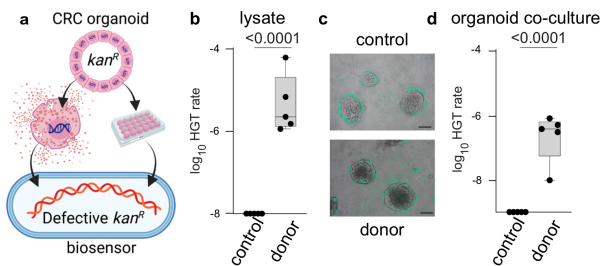


**Figure 3: Detection of donor DNA from BTRZI-*KRAS-kan<sup>R</sup>* organoids.** **a**, Schema depicting *in vitro* co-culture of *A. baylyi* sensor bacteria with BTRZI-*KRAS-kan<sup>R</sup>* (CRC donor) organoid lysates or viable organoids to assess HGT repair of kanamycin resistance gene (*kan<sup>R</sup>*). **b**, Recombination with DNA from crude lysates enables growth of *A. baylyi* sensor on kanamycin plates with transformation efficiency of  $1.4 \times 10^{-5}$  (limit of detection  $10^{-8}$ ). **c**, Representative images of GFP-tagged *A. baylyi* sensor surrounding parental BTRZI (control) and BTRZI-*KRAS-kan<sup>R</sup>* donor organoids at 24h. Scale bar 100  $\mu\text{m}$ . **d**, Co-culture of established CRC BTRZI-*KRAS-kan<sup>R</sup>* donor organoids with *A. baylyi* sensor enables growth of *A. baylyi* sensor on kanamycin plates with transformation efficiency of  $3.8 \times 10^{-7}$  (limit of detection  $10^{-9}$ ). In **b**, **d**,  $n = 5$  independent experiments each with 5 technical replicates, one sample t-test on transformed data was used for statistical analysis with P values as indicated.

the parental organoids (Fig. 3b, Extended Data Fig. 4a). Next, we co-cultured GFP-expressing sensor *A. baylyi* with BTRZI parental or BTRZI-*KRAS-kan<sup>R</sup>* donor organoids for 24 hours on Matrigel. The GFP-expressing sensor bacteria surrounded the organoids (Fig. 3c and Extended Data Fig. 4b). Following co-culture with donor, but not parental, organoids, the *A. baylyi* sensor bacteria acquired donor DNA via HGT (Fig. 3d). HGT of kanamycin resistance was confirmed by Sanger sequencing of individual colonies (Extended Data Fig. 4c). Note that these experiments did not

155 test specificity for mutant *KRAS*, but

156 whether organoid-to-bacteria HGT would occur in organoid co-culture.

157

### 158 Sensor bacteria can detect tumor DNA *in vivo*

159

160 Given that cancer to bacterial HGT occurred *in vitro*, both in cell lines and in organoid  
161 co-culture, we sought to test this system *in vivo*. *A. baylyi* previously survived transit  
162 through the mouse gastrointestinal tract in germ-free animals<sup>18</sup>. To confirm this finding  
163 and to optimize our experimental protocol, we used mCherry-expressing, kanamycin-  
164 resistant *A. baylyi*. One week after antibiotic gut decontamination, we administered  $10^{10}$   
165 *A. baylyi* either by single oral gavage or rectal enema. Mice administered *A. baylyi* by  
166 either route maintained gastrointestinal colonization for at least one week, as measured  
167 by stool CFU assays and fluorescence (Extended Data Fig. 5). Next, we confirmed that  
168 our BTRZI, orthotopic CRC model released tumoral DNA into the fecal stream. In this  
169 mouse model of CRC, engineered CRC organoids were injected orthotopically, by mouse  
170 colonoscopy, into the mouse colon to form colonic tumors, as previously described<sup>27</sup>. Using  
171 digital droplet PCR, we measured *Braf* mutant tumor DNA in stools collected from  
172 tumor-bearing and control mice. The BTRZI model reliably released tumor DNA into  
173 the colonic lumen (Extended Data Fig. 6).

174

175 Having confirmed that sensor bacteria would colonize the mouse gastrointestinal tract  
176 and that DNA is released from the tumor, we conducted an orthotopic CRC experiment  
177 (Fig. 4a). At week -4, NSG mice were either injected colonoscopically, or not, with

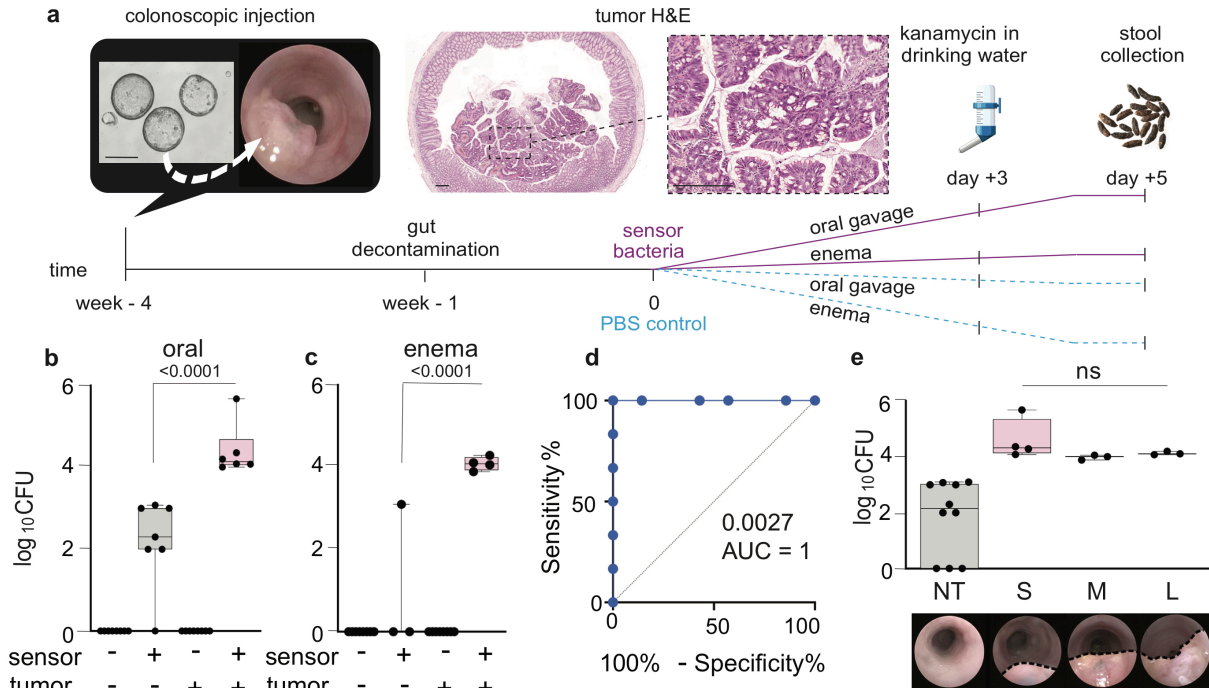


**Figure 4. Horizontal gene transfer detected in stool from mice bearing BTRZI-KRAS-kan<sup>R</sup> tumors after oral or rectal dosing of *A. baylyi* sensor bacteria.** **a** Schema depicting *in vivo* HGT experiments: generation of BTRZI-KRAS-kan<sup>R</sup> (CRC donor) tumors in mice via colonoscopic injection of CRC donor organoids with tumor pathology validated by H&E histology, administration of PBS control or sensor *A. baylyi* and stool collection. Scale bars 200 $\mu$ m. **b**, oral or **c**, rectal delivery of *A. baylyi* sensor to mice bearing CRC donor tumors results in kanamycin resistant *A. baylyi* sensor in stool via HGT. Average CFU per stool from 2-4 stools per mouse grown on Kanamycin selection plates is shown, n=3-8 mice/group. **d**, ROC curve analysis of HGT CFU following oral gavage. **e**, HGT CFU rate in stool was not affected by donor tumor size in recipient mice, as determined by colonoscopic scoring (S small, M medium, L large). In **b,c,e**, one-way Anova with Tukey's post-hoc on  $\log_{10}$  transformed data was used for statistical analysis with P values shown in the corresponding panels. Limit of detection 80 CFUs

178 BTRZI-KRAS-kan<sup>R</sup> organoids. At week -1, mice underwent a gut decontamination  
 179 regimen. A single dose of 10<sup>10</sup> “small insert” *A. baylyi* biosensors or nonengineered  
 180 parental bacteria, with additional chloramphenicol resistance for quantification of total  
 181 *A. baylyi*, was administered by oral gavage or enema to tumor-bearing and non-tumor-  
 182 bearing mice. Additional control mice with and without tumors that were administered  
 183 PBS rather than sensor bacteria were included as well (Fig. 4a). All study groups were  
 184 housed in separate cages. At day 3 after sensor bacteria delivery, mice were administered  
 185 2 days of low-dose kanamycin in their drinking water, before having their stools collected  
 186 at day 5. HGT was measured by serial dilution of stool culture on chloramphenicol and  
 187 kanamycin agar plates, with results presented as the mean CFU per 2-4 stools collected  
 188 for each mouse.

189

190 Following sensor bacteria delivery, either by oral (Fig. 4b) or rectal (Fig. 4c) delivery,  
 191 the kan-resistant CFUs were significantly higher in the tumor-bearing mice compared to  
 192 either non-tumor mice (Fig. 4b,c) or mice with tumors and parental (non-engineered) *A.*  
 193 *baylyi* (Extended Data Fig. 7). The sensor bacteria perfectly discriminated tumor from

194 non-tumor bearing mice (Fig. 4d). The mean stool CFUs were the same regardless of  
195 tumor size at the time of stool collection (Fig. 4e). HGT-mediated antibiotic resistance  
196 was confirmed by Sanger sequencing of individual colonies (Extended Data Fig. 8).  
197 Finally, to ensure that HGT was not occurring on the agar plates *ex vivo*, the collected  
198 stool was pre-treated with DNase, which did not reduce the measured CFUs (Extended  
199 Data Fig. 9).

200

## 201 Discussion

202

203 In this study, naturally competent *A. baylyi* were engineered to sense donor DNA from  
204 human tumor cells. The donor-sensor system was optimized *in vitro* and then validated  
205 *in vivo* using an orthotopic mouse model of CRC. Furthermore, we engineered a CRISPR-  
206 based technique to provide specificity for the mutant *KRASG12D* vs. wild-type *KRAS*.  
207 The sensor bacteria described here demonstrate that a living biosensor can detect tumor  
208 DNA shed from CRC *in vivo* in the gut, with no sample preparation or processing. The  
209 sensor is highly sensitive and specific, with 100% discrimination between mice with and  
210 without CRC.

211

212 *In vitro* DNA analysis helps detect and manage important human diseases, including  
213 cancer and infection<sup>28</sup>. However, *in vitro* sensing requires potentially invasive removal of  
214 samples, and many DNA diagnostics cannot achieve clinically relevant sequence  
215 resolution, with more advanced sequencing remaining too expensive for routine use in all  
216 settings<sup>29</sup>. Direct sampling of the gut *in vivo* may offer important advantages. The  
217 gastrointestinal tract contains significant DNase activity<sup>30</sup>, which limits the lifetime of  
218 free DNA in both rodents and humans<sup>18,31,32</sup>, and may thus reduce the information content  
219 of downstream fecal samples<sup>33-35</sup>. Bacterial biosensors located *in situ* could capture and  
220 preserve DNA shortly after its release, before degradation by local DNases. In addition,  
221 biosensors could amplify target DNA through HGT-induced fitness, intercellular quorum  
222 sensing circuits, or intracellular genetic memory switches<sup>9,11</sup>. Perhaps most exciting,  
223 however, is that unlike *in vitro* diagnostics, bacterial detection of target DNA could be  
224 coupled to direct and genotype-complementary nanobodies, peptides, or other small  
225 molecules for the treatment of cancer or infection<sup>36,37</sup>. The sensor may also have important  
226 applications in many other settings both clinical and non-clinical, particularly where  
227 direct sampling is difficult or too invasive, continuous surveillance is desirable, diagnostic  
228 resources are constrained, or a biologically-generated response would be best delivered to  
229 the target organism at the time and place of its detection.

230

231



232 **References**

233

- 234 1. Slomovic, S., Pardee, K. & Collins, J. J. Synthetic biology devices for in vitro and in vivo  
235 diagnostics. *Proc National Acad Sci* 112, 14429–14435 (2015).
- 236 2. Sedlmayer, F., Aubel, D. & Fussenegger, M. Synthetic gene circuits for the detection,  
237 elimination and prevention of disease. *Nat Biomed Eng* 2, 399–415 (2018).
- 238 3. Lim, W. A. & June, C. H. The Principles of Engineering Immune Cells to Treat Cancer. *Cell*  
239 168, 724–740 (2017).
- 240 4. Riglar, D. T. *et al.* Engineered bacteria can function in the mammalian gut long-term as live  
241 diagnostics of inflammation. *Nat Biotechnol* 35, 653–658 (2017).
- 242 5. Mark, M. *et al.* An ingestible bacterial-electronic system to monitor gastrointestinal health.  
243 *Science* 360, 915 (2018).
- 244 6. Mao, N., Cubillos-Ruiz, A., Cameron, D. E. & Collins, J. J. Probiotic strains detect and  
245 suppress cholera in mice. *Sci Transl Med* 10, eaao2586 (2018).
- 246 7. Danino, T. *et al.* Programmable probiotics for detection of cancer in urine. *Sci Transl Med* 7,  
247 289ra84-289ra84 (2015).
- 248 8. Dina, K. *et al.* Effect of Oral Capsule– vs Colonoscopy-Delivered Fecal Microbiota  
249 Transplantation on Recurrent *Clostridium difficile* Infection: A Randomized Clinical Trial. *Jama*  
250 318, 1985–1993 (2017).
- 251 9. Kotula, J. W. *et al.* Programmable bacteria detect and record an environmental signal in the  
252 mammalian gut. *Proc National Acad Sci* 111, 4838–4843 (2014).
- 253 10. Gardner, T. S., Cantor, C. R. & Collins, J. J. Construction of a genetic toggle switch in  
254 *Escherichia coli*. *Nature* 403, 339–342 (2000).
- 255 11. Courbet, A., Endy, D., Renard, E., Molina, F. & Bonnet, J. Detection of pathological  
256 biomarkers in human clinical samples via amplifying genetic switches and logic gates. *Sci Transl*  
257 *Med* 7, 289ra83 (2015).
- 258 12. Chang, M., Joshua & J, R., Rosemary. Natural competence and the evolution of DNA uptake  
259 specificity. *J Bacteriol* 196, 1471–1483 (2014).
- 260 13. Soucy, S. M., Huang, J. & Gogarten, J. P. Horizontal gene transfer: building the web of life.  
261 *Nature Reviews Genetics* 16, 472–482 (2015).

- 262 14. Robinson, K. M., Sieber, K. B. & Hotopp, J. C. D. A Review of Bacteria-Animal Lateral  
263 Gene Transfer May Inform Our Understanding of Diseases like Cancer. *Plos Genet* 9, e1003877  
264 (2013).
- 265 15. Hotopp, J. C. D. Horizontal gene transfer between bacteria and animals. *Trends Genet* 27,  
266 157–163 (2011).
- 267 16. Young, D. M., Parke, D. & Ornston, L. N. Opportunities for genetic investigation afforded  
268 by *Acinetobacter baylyi*, a nutritionally versatile bacterial species that is highly competent for  
269 natural transformation. *Annu Rev Microbiol* 59, 519–551 (2005).
- 270 17. Chen, T.-L. *et al.* *Acinetobacter baylyi* as a Pathogen for Opportunistic Infection ▽. *J Clin*  
271 *Microbiol* 46, 2938–2944 (2008).
- 272 18. Nordgård, L. *et al.* Lack of detectable DNA uptake by bacterial gut isolates grown in vitro  
273 and by *Acinetobacter baylyi* colonizing rodents in vivo. *Environmental Biosafety Research* 6,  
274 149–160 (2007).
- 275 19. Vogelstein, B. *et al.* Genetic Alterations during Colorectal-Tumor Development. *New Engl J*  
276 *Medicine* 319, 525–532 (1988).
- 277 20. Simpson, D. J., Dawson, L. F., Fry, J. C., Rogers, H. J. & Day, M. J. Influence of flanking  
278 homology and insert size on the transformation frequency of *Acinetobacter baylyi* BD413.  
279 *Environmental Biosafety Research* 6, 55–69 (2007).
- 280 21. Cooper, R. M., Tsimring, L. & Hasty, J. Inter-species population dynamics enhance  
281 microbial horizontal gene transfer and spread of antibiotic resistance. *eLife* 6, 8053 (2017).
- 282 22. Palmen, R., Vosman, B., Buijsman, P., Breek, C. K. D. & Hellingwerf, K. J. Physiological  
283 characterization of natural transformation in *Acinetobacter calcoaceticus*. *Microbiology+* 139,  
284 295–305 (1993).
- 285 23. Consortium, T. A. P. G. AACR Project GENIE: Powering Precision Medicine through an  
286 International Consortium. *Cancer Discov* 7, 818–831 (2017).
- 287 24. Priestley, P. *et al.* Pan-cancer whole-genome analyses of metastatic solid tumours. *Nature*  
288 575, 210–216 (2019).
- 289 25. Cooper, R. M. & Hasty, J. One-Day Construction of Multiplex Arrays to Harness Natural  
290 CRISPR-Cas Systems. *Acs Synth Biol* 9, 1129–1137 (2020).
- 291 26. van de Wetering, M. *et al.* Prospective Derivation of a Living Organoid Biobank of  
292 Colorectal Cancer Patients. *Cell* 161, 933–945 (2015).
- 293 27. Lannagan, T. R. M. *et al.* Genetic editing of colonic organoids provides a molecularly  
294 distinct and orthotopic preclinical model of serrated carcinogenesis. *Gut* 68, 684–692 (2018).

- 295 28. Zhong, Y., Xu, F., Wu, J., Schubert, J. & Li, M. M. Application of Next Generation  
296 Sequencing in Laboratory Medicine. *Ann Lab Med* 41, 25–43 (2021).
- 297 29. Iwamoto, M. *et al.* Bacterial enteric infections detected by culture-independent diagnostic  
298 tests--FoodNet, United States, 2012-2014. *Mmwr Morbidity Mortal Wkly Rep* 64, 252–7 (2015).
- 299 30. Shimada, O. *et al.* Detection of Deoxyribonuclease I Along the Secretory Pathway in Paneth  
300 Cells of Human Small Intestine. *J Histochem Cytochem* 46, 833–840 (1998).
- 301 31. Wilcks, A., Hoek, A. H. A. M. van, Joosten, R. G., Jacobsen, B. B. L. & Aarts, H. J. M.  
302 Persistence of DNA studied in different ex vivo and in vivo rat models simulating the human gut  
303 situation. *Food Chem Toxicol* 42, 493–502 (2004).
- 304 32. Netherwood, T. *et al.* Assessing the survival of transgenic plant DNA in the human  
305 gastrointestinal tract. *Nat Biotechnol* 22, 204–209 (2004).
- 306 33. Imperiale, T. F. *et al.* Multitarget Stool DNA Testing for Colorectal-Cancer Screening. *New*  
307 *England Journal of Medicine* 370, 1287–1297 (2014).
- 308 34. Zmora, N. *et al.* Personalized Gut Mucosal Colonization Resistance to Empiric Probiotics Is  
309 Associated with Unique Host and Microbiome Features. *Cell* 174, 1388-1405.e21 (2018).
- 310 35. Tang, Q. *et al.* Current Sampling Methods for Gut Microbiota: A Call for More Precise  
311 Devices. *Front Cell Infect Mi* 10, 151 (2020).
- 312 36. Din, M. O. *et al.* Synchronized cycles of bacterial lysis for in vivo delivery. *Nature* 536, 81–5  
313 (2016).
- 314 37. Sepich-Poore, G. D. *et al.* The microbiome and human cancer. *Science* 371, eabc4552  
315 (2021).

316  
317  
318  
319

320 **Figure legends**

321

322 **Figure 1. Engineered bacteria to detect tumor DNA.** Engineered *A. baylyi*  
323 bacteria are delivered orally or rectally in an orthotopic mouse model of CRC. The  
324 naturally competent *A. baylyi* take up tumor DNA shed into the colonic lumen. The  
325 tumor donor DNA is engineered with a *kan<sup>R</sup>* cassette flanked by *KRAS* homology arms  
326 (HA). The sensor bacteria are engineered with matching *KRAS* homology arms that  
327 promote homologous recombination. Sensor bacteria that undergo HGT from tumor DNA  
328 acquire kanamycin resistance and are quantified from stool by serial dilution on  
329 kanamycin selection plates.

330

331 **Figure 2: Sensing *KRASG12D* DNA *in vitro*.** **a-c)** Donor DNA consisting of  
332 plasmid, purified cancer cell genomic DNA, or raw lysate (top) recombines into biosensor  
333 *A. baylyi* cells (bottom), transferring either a large, 2 kb insert (**b**), or a small, 8 bp insert  
334 to repair 2 stop codons (**c**), in both cases conferring kanamycin resistance. **d-g)** *A. baylyi*  
335 biosensors were incubated with plasmid DNA, purified RKO-*KRAS* or LS174T-*KRAS*  
336 genomic DNA, or raw RKO-*KRAS* lysate, all containing the donor cassette, or purified  
337 RKO or LS174T genomic DNA as controls. Biosensor cells included either “large insert”  
338 (**b,d,e**) or “small insert” (**c,f,g**) designs, and transformations were performed in liquid  
339 culture (**d,f**) or on solid agar surfaces (**e,g**). Two-sample t-tests compared data to  
340 combined RKO and LS174T genomic DNA controls for the same conditions. **h)** CRISPR  
341 spacers targeting the *KRAS* G12D mutation (boxed), using the underlined PAMs. **i,j)**  
342 Fraction of total biosensor cells expressing the indicated CRISPR spacers that were  
343 transformed by plasmid donor DNA with wild type (**i**) or mutant G12D (**j**) *KRAS*.  
344 Statistics were obtained using two-sample, one-sided t-tests. Data points below detection  
345 are shown along the x-axis, at the limit of detection.

346

347 **Figure 3: Detection of donor DNA from BTRZI-*KRAS-kan<sup>R</sup>* organoids.**

348 Schema depicting *in vitro* co-culture of *A. baylyi* sensor bacteria with BTRZI-*KRAS-*  
349 *kan<sup>R</sup>* (CRC donor) organoid lysates or viable organoids to assess HGT repair of kanamycin  
350 resistance gene (*kan<sup>R</sup>*). **b.** Recombination with DNA from crude lysates enables growth of  
351 *A. baylyi* sensor on kanamycin plates with transformation efficiency of  $1.4 \times 10^{-5}$  (limit of  
352 detection  $10^{-8}$ ). **c.** Representative images of GFP-tagged *A. baylyi* sensor surrounding  
353 parental BTRZI (control) and BTRZI-*KRAS-kan<sup>R</sup>* donor organoids at 24h. Scale bar  
354 100 $\mu$ m **d.** Co-culture of established CRC BTRZI-*KRAS-kan<sup>R</sup>* donor organoids with *A.*  
355 *baylyi* sensor enables growth of *A. baylyi* sensor on kanamycin plates with transformation  
356 efficiency  $3.8 \times 10^{-7}$  (limit of detection  $10^{-9}$ ). In **b, d**,  $n = 5$  independent experiments each

357 with 5 technical replicates, one sample t-test on transformed data was used for statistical  
358 analysis with *P* values as indicated.

359

360 **Figure 4. Horizontal gene transfer detected in stool from mice bearing BTRZI-**  
361 ***KRAS-kan<sup>R</sup>* tumors after oral or rectal dosing of *A. baylyi* sensor bacteria. **a,****  
362 Schema depicting *in vivo* HGT experiments: generation of BTRZI-*KRAS-kan<sup>R</sup>* (CRC  
363 donor) tumors in mice, administration of PBS control or sensor *A. baylyi* and stool  
364 collection. Scale bars 200µm. **b,** oral or **c,** rectal delivery of *A. baylyi* sensor to mice  
365 bearing CRC donor tumors results in kanamycin resistant *A. baylyi* sensor in stool via  
366 HGT. Average CFU per stool from 2-4 stools per mouse grown on Kanamycin selection  
367 plates is shown, n=3-8 mice/group. **d,** ROC curve analysis of HGT CFU following oral  
368 gavage. **e,** HGT CFU rate in stool was not affected by donor tumor size in recipient mice,  
369 as determined by colonoscopic scoring (S small, M medium, L large). In **b,c,e,** one-way  
370 Anova with Tukey's post-hoc on log10 transformed data was used for statistical analysis  
371 with *P* values shown in the corresponding panels. Limit of detection 80 CFUs.

372

373



374 **Methods**

375

376 **Data availability**

377 All data generated or analyzed during this study are included in this published article  
378 (and its supplementary information files), and raw data files are available upon request.

379

380 **Bacterial cell culture and cloning to generate biosensors**

381 *Acinetobacter baylyi* ADP1 was obtained from the American Type Culture Collection  
382 (ATCC #33305) and propagated in standard LB media at 30 or 37 °C. *KRAS* homology  
383 arms were inserted into a neutral genetic locus denoted *Ntrl1*, replacing the gene remnant  
384 ACIAD2826. For the “large insert” design, a spectinomycin resistance gene was placed  
385 between the *KRAS* homology arms. For the “small insert” design, two stop codons were  
386 placed near the beginning of the *kan<sup>R</sup>* gene of the donor cassette, and the broken cassette  
387 was inserted into *A. baylyi*. CRISPR arrays were inserted into a neutral locus used  
388 previously, replacing ACIAD2186, 2187 and part of 2185. Ectopic CRISPR arrays were  
389 driven by a promoter region that included 684 bp from upstream of the first repeat of the  
390 endogenous, 90-spacer array.

391

392 ***In vitro* biosensor transformation experiments**

393 *A. baylyi* were grown overnight in LB at 30 °C. Cells were then washed, resuspended in  
394 an equal volume of fresh LB, and mixed with donor DNA. For transformation in liquid,  
395 50 µl cells were mixed with 250 ng donor DNA and incubated in a shaker at 30 °C for 2  
396 hours or overnight. For transformation on agar, 2 µl cells were mixed with >50 ng donor  
397 DNA, spotted onto LB plates containing 2% wt/vol agar, and incubated at 30 °C  
398 overnight. Spots were cut out the next day and resuspended in 500 µl phosphate buffered  
399 saline solution (PBS). To count transformants, cells were 10-fold serially diluted 5 times,  
400 and 2 µl spots were deposited onto selective (30 ng/ml kanamycin) and non-selective 2%  
401 agar plates, with 3 measurement replicates at each dilution level. Larger volumes of  
402 undiluted samples were also spread onto agar plates to increase detection sensitivity (25  
403 µl for liquid culture, 100 µl for resuspended agar spots). Colonies were counted at the  
404 lowest countable dilution level after overnight growth at 30 °C, and measurement  
405 replicates were averaged. Raw, unpurified lysate was produced by growing donor RKO  
406 cells in a culture dish until confluence, trypsinizing and harvesting cells, pelleting them in  
407 a 15 ml tube, resuspending them in 50 µl PBS, and placing the tube in a -20 °C freezer  
408 overnight to disrupt cell membranes.

409

410 ***In vitro* statistics**

411 Hypothesis testing was performed using 2-sample, one-sided t-tests in Matlab after taking  
412 base 10 logarithms, since serial dilutions produce log-scale data. Where data points were  
413 below the limit of detection, they were replaced by the limit of detection as the most  
414 conservative way to include them in log-scale analysis. Comparisons between large vs  
415 small inserts or liquid vs solid agar culture were performed using paired t-tests, where  
416 data were matched for donor DNA and either culture type (liquid vs agar) or insert size,  
417 respectively. For Figure 2, d-g) n=4, i,j) n=5 except for random spacer n=3.

418

#### 419 **Creation of BTRZI CRC donor organoids**

420 BTRZI (Braf<sup>V600E</sup>;Tgfbr2<sup>Δ/Δ</sup>;Rnf43<sup>Δ/Δ</sup>/Znf43<sup>Δ/Δ</sup>;p16 Ink4a<sup>Δ/Δ</sup>) organoids were generated  
421 using CRISPR-Cas9 engineering (Lannagan et al, 2019 Gut) and grown in 50 μl domes of  
422 GFR-Matrigel (Corning,; 356231) in organoid media: Advanced Dulbecco's modified Eagle  
423 medium/F12 (Life Technologies) supplemented with 1x  
424 gentamicin/antimycotic/antibiotic (Life Technologies), 10mM HEPES (Gibco), 2 mM  
425 GlutaMAX (Gibco), 1x B27 (Life Technologies; 12504-044), 1x N2 (Life Technologies;  
426 17502048), 50 ng/ml mouse recombinant EGF (Peprotech; 315-09), 10 ng/ml human  
427 recombinant TGF-β1 (Peprotech; 100-21). Following each split, organoids were cultured  
428 in 10 μM Y-27632 (MedChemExpress; HY-10583), 3 μM iPSC (Calbiochem; 420220), 3  
429 μM GSK-3 inhibitor (XVI, Calbiochem; 361559) for the first 3 days.

430 To create BTRZI CRC donor organoids, lentiviral expression plasmid pD2119-FLuc2  
431 KRasG12D donor was co-transfected with viral packaging vectors, psPAX2 (Addgene;  
432 plasmid; 12260) and MD2G (Addgene; plasmid; 12259), into HEK293T cells. At 48 and  
433 72 h after transfection, viral supernatants were harvested, filtered through a 0.45-μm  
434 filter, and concentrated using Amicon Ultra Centrifugal Filters (Merck Millipore;  
435 UFC910024). Concentrated lentivirus particles were used for transduction. The viral  
436 supernatant generated was used to transduce BTRZI organoids by spinoculation. Briefly,  
437 organoids were dissociated to single cells using TrypLE. 1x10<sup>5</sup> single cells were mixed with  
438 250 μl organoid media; 10 μM Y-27632; 250 μl concentrated viral supernatant and 4 μg/ml  
439 polybrene (Sigma,; H9268) in a 48 well tray before centrifugation at 600 xg for 90 minutes  
440 at 32 °C. Meanwhile, 120 μl 50:50 ADMEM:Matrigel mixture was added to a cold 24-well  
441 tray before centrifugation of this bottom matrigel layer for 40 minutes at 200xg at room  
442 temperature, followed by solidifying the Matrigel by incubating at 37 °C for 30 minutes.  
443 After spinoculation, cells were scraped from the well and plated on top of the Matrigel  
444 monolayer with organoid media. The following day, the media was removed and the upper  
445 layer of Matrigel was set over the organoids by adding 120 μl 50:50 ADMEM:Matrigel  
446 and allowing to set for 30 minutes before adding organoid media. 48 hours after  
447 transduction, BTRZI donor organoids were selected with 8 μg/ml puromycin for 1 week,  
448 then maintained in organoid media with 4 μg/ml puromycin.

449

#### 450 **Organoid lysate mixed with *A. baylyi* sensor bacteria**

451 BTRZI (parental) and BTRZI donor organoids were grown for 5 days in 50 ml Matrigel  
452 domes. Organoids were dissociated to single cells with TrypLE, counted and 6x10<sup>5</sup> single  
453 cells were collected in PBS and snap frozen. The CFU equivalence of exponentially  
454 growing *A. baylyi* sensor culture at OD<sub>600</sub> 0.35 was ascertained by serial dilution of 3  
455 independent cultures with 5 technical replicates plated on 10 μg/ml Chloramphenicol LB  
456 agar plate to be 2.4 x 10<sup>8</sup> CFU per ml. *A. baylyi* sensor was grown in liquid culture with

457 10 µg/ml Chloramphenicol to OD<sub>600</sub> 0.35 before mixing with organoid lysate at a 1:1 ratio  
458 and grow overnight on LB agar plates at 30 °C. All bacteria was scraped into 200 µl  
459 LB/20% glycerol before spotting 5x 5 µl spots onto kanamycin and chloramphenicol plates  
460 and grown overnight at 37 °C. Colonies were counted and the dilution factor was  
461 accounted for to calculate CFU per ml. Rate of HGT was calculated by dividing the CFU  
462 per ml of transformants (Kanamycin plates) by the CFU per of total *A. baylyi*  
463 (chloramphenicol plates) for 5 independent experiments.

464

#### 465 **Coculture organoids with *A. baylyi* sensor bacteria**

466 For co-culture experiments, 24-well trays were coated with Matrigel monolayers. Briefly,  
467 200 µl 50:50 ADMEM:Matrigel mixture was added to a cold 24-well tray and centrifuged  
468 for 40 minutes at 200xg at room temperature, followed by a 30 minute incubation at 37  
469 °C to solidify matrigel. BTRZI (parental) and BTRZI donor organoids were dissociated  
470 into small clusters using TrypLE and grown for 5 days on a Matrigel monolayer in  
471 organoid media without antibiotics before 50 µl OD<sub>600</sub> 0.35 *A. baylyi* sensor was added to  
472 each well. After 24 hours, organoids were photographed then collected and grown  
473 overnight on LB agar plates at 30 °C. All bacteria was scraped into 200 µl LB/20%  
474 glycerol before spotting 5x 5 µl spots onto kanamycin and chloramphenicol plates and  
475 grown overnight at 37 °C. Colonies were counted and the dilution factor was accounted  
476 for to calculate CFU per ml. Rate of HGT was calculated by dividing the CFU per ml of  
477 transformants (kanamycin plates) by the CFU per ml of total *A. baylyi* (chloramphenicol  
478 plates) for 5 independent experiments.

479

#### 480 ***A. baylyi* colonisation trial**

481 This study was approved by the SAHMRI Animal Ethics committee (SAM20.036).  
482 NOD.Cg-*Prkdc*<sup>scid</sup>*Il2rg*<sup>tm1Wjl</sup>/SzJ (NSG) mice (male and female, 10-13 weeks old) were  
483 obtained from the SAHMRI Bioresources facility and housed under pathogen-free  
484 conditions. NSG mice were administered with antibiotics (2.7mM Ampicillin, Sigma;  
485 A1066 and 0.55mM Neomycin, Sigma; N1876) in drinking water a week prior to oral  
486 gavage/enema. *A. baylyi*-mCherry/KanR was grown in liquid culture with 50 µg/ml  
487 kanamycin to OD<sub>600</sub> 0.3. *A. baylyi* was washed with PBS before 3 mice received 10<sup>10</sup> *A.*  
488 *baylyi* via oral gavage, 3 mice received 10<sup>10</sup> *A. baylyi* via enema and 2 control mice received  
489 PBS (1x enema and 1x oral gavage). Oral gavage was administered using a 20G curved  
490 feeding needle at a volume of 200 µl per mouse. Enema was performed as per previous  
491 publication. Briefly, mice were anaesthetised with isoflurane and colon flushed with 1 ml  
492 of room temperature sterile PBS to clear the colon cavity of any remaining stool. A P200  
493 pipette tip coated with warm water was then inserted parallel into the lumen to deliver  
494 50 mL of bacteria into the colon over the course of 30 seconds. After infusion, the anal

495 verge was sealed with Vetbond Tissue Adhesive (3M; 1469SB) to prevent luminal contents  
496 from being immediately excreted. Animals were maintained on anaesthesia for 5 minutes,  
497 and then allowed to recover on heat mat and anal canal inspected 6 hours after the  
498 procedure to make sure that the adhesive has been degraded. Stool was collected for 2  
499 weeks in 250  $\mu$ l PBS/20% glycerol, vortexed and stored at -80 °C. Stool slurry (50  $\mu$ l)  
500 was plated onto a LB agar plate and grown overnight at 37 °C. All bacteria was scraped  
501 into 200  $\mu$ l LB/20% glycerol. 5x 5 $\mu$ l serial dilutions were spotted onto kanamycin plates.  
502 Colonies were counted and dilutions were factored to calculate CFU *A. baylyi* per stool.  
503

#### 504 **Horizontal gene transfer *in vivo***

505 BTRZI donor organoids were isolated from Matrigel and dissociated into small clusters  
506 using TrypLE. The cell clusters (equivalent to ~150 organoids per injection) were  
507 washed three times with cold PBS containing 10  $\mu$ M Y-27632 and then resuspended in 20  
508  $\mu$ l 10% GFR matrigel 1:1000 india ink, 10  $\mu$ M Y-27632 in PBS and orthotopically injected  
509 into the mucosa of the proximal and distal colon of anaesthetised 10-13 week old NSG  
510 mice (150 organoids per injection), as previously described (Lannagan et al, 2019 Gut).  
511 Briefly, a customised needle (Hamilton Inc. part number 7803-05, removable needle, 33  
512 gauge, 12 inches long, point 4, 12 degree bevel) was used. In each mouse up to 2 injections  
513 of 20 $\mu$ l were performed. CRC donor tumor growth was monitored by colonoscopy for 4  
514 weeks and the videos were viewed offline using QuickTime Player for analysis.  
515 Colonoscopy was performed using a Karl Storz Image 1 Camera System comprised of:  
516 Image1 HDTV HUB CCU; Cold Light Fountain LED Nova 150 light source; Full HD  
517 Image1 3 Chip H3-Z Camera Head; Hopkins Telescope, 1.9mm, 0 degrees. A sealed luer  
518 lock was placed on the working channel of the telescope sheath to ensure minimal air  
519 leakage (Coherent Scientific, # 14034-40). Tumor growth of the largest tumor visualised  
520 was scored as previously described using the Becker Scale (Rex et al, 2012 Am J  
521 Gastroenterol). Mice were administered antibiotics (2.7mM Ampicillin, Sigma; A1066 and  
522 0.55mM Neomycin, Sigma; N1876) in drinking water a week prior to oral gavage/enema.  
523 *A. baylyi* sensor was grown in liquid culture with 10  $\mu$ g/ml Chloramphenicol to OD<sub>600</sub> 0.3.  
524 *A. baylyi* sensor was washed with PBS before 13 mice received 10<sup>10</sup> *A. baylyi* sensor via  
525 oral gavage (7 mice without tumors and 6 mice with CRC donor tumors), 7 mice received  
526 10<sup>10</sup> *A. baylyi* sensor via enema (3 mice without tumors and 4 mice with CRC donor  
527 tumors). Three days after *A. baylyi* administration, mice received 10 mg/L kanamycin in  
528 their drinking water, except 2 mice from the oral gavage *A. baylyi* sensor, CRC donor  
529 tumor cohort, 5 mice from the oral gavage *A. baylyi* sensor, no tumor cohort and 2 mice  
530 from the enema *A. baylyi* sensor, no tumor cohort . Stool was collected 5 days after *A.*  
531 *baylyi* administration into 250  $\mu$ l PBS/20% glycerol, vortexed and stored at -80 °C. Stool  
532 slurry (50  $\mu$ l) was plated onto a LB agar plate and grown overnight at 37 °C. All bacteria

533 was scraped into 200  $\mu$ l LB/20% glycerol. 5x 5 $\mu$ l serial dilutions were spotted onto  
534 chloramphenicol and kanamycin plates. Colonies were counted and dilutions were factored  
535 to calculate CFU *A. baylyi* per stool.

536

### 537 **Sequencing gDNA from bacterial colonies grown on kanamycin plates**

538 *A. baylyi* transformants were individually picked from kanamycin plates and grown in  
539 liquid culture LB supplemented with 25  $\mu$ g/ml Kanamycin. gDNA was extracted using  
540 purelink genomic DNA minikit (Invitrogen; K182001). Genomic regions of interest were  
541 amplified using Primestar Max DNA polymerase (Takara, # R045A) and primers  
542 HGT<sub>pcr</sub>F: CAAAATCGGCTCCGTCGATACTA;  
543 HGT<sub>pcr</sub>R: TAGCATCACCTTCACCCTC;  
544 Kan seqF: AAAGATACGGAAGGAATGTCTCC;  
545 Kan seqR: CGGCCGTCTAAGCTATTCGT. Sanger sequencing was conducted by  
546 AGRF using the same primers.

547

### 548 **DNase treatment of stool**

549 Stool slurry (25  $\mu$ l) was mixed with 2.5  $\mu$ l 10x DNase 1 buffer with or without 1  $\mu$ l DNase  
550 1 (2.7 U/ $\mu$ l) using RNase-free DNase 1 kit (Qiagen,; 79254). Samples were incubated at  
551 37 °C for 30 minutes then the mixture was plated onto LB agar plates and grown overnight  
552 at 37 °C. A control to assess DNase 1 activity was set up simultaneously with 25  $\mu$ l stool  
553 (from mouse with no tumor); 1  $\mu$ l 100 ng/ $\mu$ l KRasG12D donor plasmid DNA (2 ng/ $\mu$ l  
554 final concentration); 2.5  $\mu$ l 10x DNase 1 buffer with or without 1  $\mu$ l DNase 1 (2.7 U/ $\mu$ l),  
555 which was incubated at 37 °C for 30 minutes. Following DNase 1 treatment, controls were  
556 mixed with 25  $\mu$ l of *A. baylyi* sensor liquid culture (OD<sub>600</sub> 0.35) and incubated at 37 °C 2  
557 hrs before the mixture was plated onto LB agar plates and grown overnight at 37 °C. All  
558 bacteria was scraped into 200  $\mu$ l LB/20% glycerol. 5x 5 $\mu$ l serial dilutions were spotted  
559 onto kanamycin plates. Colonies were counted and dilutions were factored to calculate  
560 CFU *A. baylyi* per stool.

561



562 **Acknowledgements:** Mr Phil Winning for design assistance with Figure 1. This work  
563 was supported by NIH grant R01CA241728. **Professor Barbara Leggett and A/Prof.**  
564 **Vicki Whitehall for the original gift of the parental RKO and LS174T human**  
565 CRC cell lines used in this study.

566  
567 **Author contributions:** RC, DW & JH conceived of the concept and study plan. RC,  
568 JW, JN, JG, NS, YL, MI, GR, ET, LV, SW, DW, & JH were all involved with data  
569 acquisition and or interpretation. RC, JW, RK, SW, DW, & JH were involved in writing  
570 and revising the final manuscript.

571  
572 **Competing interest declaration:** J.H. is a co-founder and board member with equity  
573 in GenCirq Inc, which focuses on cancer therapeutics.

574  
575 **Correspondence:** Correspondence and requests for materials should be addressed to:  
576 Professor Jeff Hasty: [hasty@ucsd.edu](mailto:hasty@ucsd.edu)  
577 Associate Professor Daniel Worthley: [dan@colonoscopyclinic.com.au](mailto:dan@colonoscopyclinic.com.au)  
578 Dr Susan Woods: [susan.woods@adelaide.edu.au](mailto:susan.woods@adelaide.edu.au)

579  
580 Reprints and permissions information is available at [www.nature.com/reprints](http://www.nature.com/reprints)

## 581 582 **Extended Data**

583  
584 **Extended Data Figure 1:** Plasmid donor DNA used to transfect mammalian cell lines  
585 and as positive control donor DNA for *in vitro* experiments.

586  
587 **Extended Data Figure 2:** “Large insert” (a) and “small insert (b) designs for the  
588 biosensors. *KRAS* homology arms are shown in striped gray with surrounding genomic  
589 context outside them. Note that large and small inserts refers to the size of the donor  
590 DNA region that must transfer to confer kanamycin resistance, not to the size of the  
591 region between homology arms in the biosensor. Two single-base changes introducing  
592 nearby stop codons at the beginning of *kan<sup>r</sup>* are shown for the small insert design (b).

593  
594 **Extended Data Figure 3: "Small insert" biosensor design.** Donor DNA in the  
595 cancer cell genome (top) contains a kanamycin resistance gene *kanR*, surrounded by GFP  
596 and human *KRAS* homology arms of about 1 kb (*KRAS* HA). The bacterial biosensor  
597 genome contains the exact same construct, except that 2 stop codons are introduced to  
598 *kan<sup>r</sup>* with 2 single-base mutations within 8 bases. Upon homologous recombination with

599 the donor DNA, the 2 stop codons are repaired, and the biosensors acquire kanamycin  
600 resistance.

601

602 **Extended Data Figure 4: Sensor detection of donor DNA from BTRZI CRC**  
603 **organoids.** *A. baylyi* sensor bacteria are constitutively chloramphenicol resistant, hence  
604 *chlOR* CFUs provide a read-out of total *A. baylyi* present. In contrast, kanamycin  
605 resistant sensor bacteria rely on incorporation of donor DNA from CRC organoids to  
606 correct the defective *kan* gene and enable growth on kanamycin selection plates. **a**  
607 Recombination with lysate from CRC donor organoids enables growth of *A. baylyi* sensor  
608 on kanamycin plates. Shown here with representative plates and CFU analysis. **b** After  
609 co-culturing established CRC donor organoids with *A. baylyi* sensor, recombination with  
610 donor DNA from CRC donor organoids enables growth of *A. baylyi* sensor on kanamycin  
611 plates. Shown here with representative images and CFU analysis. Scale bars 200  $\mu$ m. **a,**  
612 **b,** Fig 3 contains the same data as shown here but presented as HGT rate (kanamycin  
613 resistant CFU *A. baylyi* per ml/chloramphenicol CFU *A. baylyi* per ml),  $n = 5$  independent  
614 experiments each with 5 technical replicates. **c** Representative Sanger sequencing  
615 chromatograms of PCR amplicon covering the region of the *kan* gene containing  
616 informative SNPs, to highlight the difference in sequence in gDNA isolated from parental  
617 *A. baylyi* sensor bacteria compared to *A. baylyi* colonies isolated from kanamycin plates  
618 following mixing with donor organoid lysates or viable organoids.

619

620 **Extended Data Figure 5: *A. baylyi* is detected in stool for 2 weeks after oral**  
621 **gavage or enema.** **a,** Schematic illustrating the experimental pipeline of colonisation  
622 trial,  $n=6$  mice administered *A. baylyi* mCherry-*kanR* bacteria (constitutively kanamycin  
623 resistant),  $n=2$  PBS control mice. Representative bright-field and fluorescent image of  
624 *A. baylyi* mCherry-*kanR* CFU from stool. **b,** *A. baylyi* mCherry-*kanR* is detected in stool  
625 from mice. Data points represent the average CFU per stool grown on kanamycin  
626 selection plates from 1-3 stools/mouse, with results from each mouse (84.2a, 84.2b, 84.2c,  
627 84.2g) plotted separately.

628

629 **Extended Data Figure 6: High sensitivity digital droplet PCR (ddPCR)**  
630 **detection of CRC mutation (*BrafV600E*) in stool DNA isolated from tumour**  
631 **bearing animals ( $n=3-4$  mice/group).** **a,** Representative images of ddPCR data. **b,**  
632 CRC mutation (*BrafV600E*) positive droplets as a % of total droplets. Analysis of no  
633 template negative control samples and stool DNA samples from non-tumour bearing  
634 animals was used to determine the sensitivity threshold of the assay. Positive control  
635 samples contain 10% *BrafV600E* gDNA spiked into stool DNA sample from non-tumour

636 bearing animal. NT, no tumour; Ts, small tumour; Tm, medium tumour; Tl, large  
637 tumour; NTC, no template PCR negative control.

638

639 **Extended Data Figure 7: Efficient horizontal gene transfer detected in stool**  
640 **from tumor bearing mice requires both engineered biosensor bacteria, as**  
641 **opposed to parental *A. baylyi*, and tumor.** Average CFU per stool from 2-4 stools  
642 per mouse grown on kanamycin selection plates is shown, n=4-10 mice/group. Combined  
643 data for oral and rectal dosing of biosensors. One-way Anova with Tukey's post-hoc on  
644 log<sub>10</sub> transformed data was used for statistical analysis with P values shown in the  
645 corresponding panel.

646

647 **Extended Data Figure 8: *A. baylyi* sensor in stool from mice bearing BTRZI**  
648 **CRC donor tumors become kanamycin resistant via HGT. a,** Representative  
649 Sanger sequencing chromatograms of PCR amplicon covering the region of the *kan* gene  
650 containing informative SNPs, to highlight the difference in sequence in parental *A. baylyi*  
651 sensor bacteria (defective *kanR*) in comparison to colonies isolated from kanamycin plates  
652 from stool of tumor bearing mice administered *A. baylyi* sensor bacteria (corrected *kanR*  
653 oral and rectal). **b** Representative CFU plates.

654

655 **Extended Data Figure 9: DNase treatment of stool homogenates to remove**  
656 **unincorporated donor DNA prior to CFU analysis did not alter number of *A.***  
657 ***baylyi* sensor bacteria that were kanamycin resistant.** Stools from mice bearing  
658 BTRZI donor tumors and administered *A. baylyi* sensor bacteria were incubated with  
659 and without DNase before CFU analysis on kanamycin plates. 1-4 stools from 5 mice  
660 were analysed. No statistical difference was evident between the number of kanamycin  
661 resistant colonies from CRC donor tumor stools treated with or without DNase. As a  
662 positive control for DNase treatment efficacy, stool from a non-tumour bearing mouse  
663 was mixed with *A. baylyi* sensor and CRC donor plasmid, then treated with or without  
664 DNase. In this case, kanamycin resistant colonies were only evident in the absence of  
665 DNase. This suggests that the HGT evident in stool from the experimental animals likely  
666 occurred *in vivo* or in stools, but prior to CFU plating. Paired t-test was used for  
667 statistical analysis.

668

669 **Extended Data Movie 1: *A. baylyi* biosensors taking up plasmid donor DNA.**

670 *A. baylyi* were grown overnight, washed into fresh LB, mixed with saturating pLenti-  
671 KRAS donor DNA, and sandwiched between an agar pad and a glass bottom dish. Images

672 were taken every 10 minutes. GFP fluorescence indicates that the cells have taken up and  
673 genomically integrated the donor DNA cassette.

674

675 **Extended Data DNA Files:**

676 DNA cassettes and surrounding regions corresponding to the “large insert” and “small  
677 insert” designs for

678 *A. baylyi*, and the plasmid donor DNA, as shown in Extended Data 1,2, in Genbank  
679 format.